An atmospheric pressure plasma source

Jaeyoung Park, I. Henins, H. W. Herrmann, G. S. Selwyn, J. Y. Jeong et al.

Additional information on Appl. Phys. Lett.

An atmospheric pressure plasma source

Jaeyoung Park,[a] I. Henins, H. W. Herrmann, and G. S. Selwyn
Plasma Physics, Los Alamos National Laboratory, Los Alamos, New Mexico 87545

J. Y. Jeong and R. F. Hicks
Chemical Engineering Department, University of California, Los Angeles, California 90095

D. Shim and C. S. Chang
New York University, New York, New York 10012 and KAIST, Taejeon, Korea

An atmospheric pressure plasma source operated by radio frequency power has been developed. This source produces a unique discharge that is volumetric and homogeneous at atmospheric pressure with a gas temperature below 300 °C. It also produces a large quantity of oxygen atoms, $\sim 5 \times 10^{15} \, \mathrm{cm}^{-3}$, which has important value for materials applications. A theoretical model shows electron densities of $0.2 - 2 \times 10^{11} \, \mathrm{cm}^{-3}$ and characteristic electron energies of 2–4 eV for helium discharges at a power level of 3–30 $\mathrm{W \, cm}^{-3}$. © *2000 American Institute of Physics.* [S0003-6951(00)01303-6]

Low-pressure plasmas have a dominant and long-established role in processing of materials ranging from silicon wafers to magnetic storage disks and thin film coatings. This is because of the unmatched capability of low pressure plasma devices in providing a vast array of chemically active species, selectable ion flux, low gas temperature, and high, uniform reaction rate over a relatively large area.[1] Yet, a major limitation of this technology is the requirement for vacuum operation which necessitates the use of expensive and complicated vacuum systems and limits the materials processing capability to high-value, vacuum-compatible materials.

In principle, atmospheric pressure plasma devices can provide a crucial advantage over low pressure plasmas because they eliminate complications introduced by the need for vacuum. For example, atmospheric pressure discharges have been used for a number of applications such as high temperature materials processing and ozone production for water purification. To date, however, the use of atmospheric pressure discharges for materials applications has not been widely realized, compared to low pressure plasmas. This is because of the high gas temperature in the discharge,[2] or the limited production of chemically active species due to localization of the discharge and/or input power limitations.[3–7]

In this report, we describe an atmospheric pressure plasma source that has shown promise to replace low pressure plasmas in some materials applications and to create applications.[8] An atmospheric pressure plasma jet (APPJ) employs a capacitively coupled electrode design and produces a stable discharge at atmospheric pressure using 13.56 MHz radio frequency (rf) power and helium feedgas. The APPJ operates without a dielectric cover over the electrode, yet produces a homogeneous discharge free from filaments, streamers, and arcing that are often observed in other atmospheric pressure discharges. The gas temperature of the discharge is typically between 50 and 300 °C. Thus, thermal

damage to treated materials can be easily avoided. Typically a small fraction (0.5%–3%) of reactive gases, e.g., oxygen or carbon tetrafluoride, is added to the helium feedgas in order to generate chemically active species. So far, the APPJ has been used to successfully etch polyimide, tungsten, tantalum, and silicon dioxide and to deposit silicon dioxide films at rates comparable to those achieved in low pressure discharge systems.[9–11] Furthermore, we have successfully tested the APPJ for decontamination of chemical and biological warfare agents using surrogates of mustard blister agent, VX nerve agent and anthrax spores.[12]

As shown in Fig. 1(a) experiments were performed using two planar aluminum electrodes, 10 cm wide and 10 cm long. The gap spacing between the rf electrode and the grounded electrode was kept at 0.16 cm using quartz spacers on both sides of the electrodes, which also provided optical access to the discharge region. The x axis denotes the direction of the gas flow and the z axis denotes the direction normal to the electrode surface. Either pure helium or helium mixed with a minority flow of O_2 was fed into the discharge region (at $x = 0$) through a series of uniformly spaced small holes (ϕ of 0.08 mm) at a flow rate of 50 slpm. It is noted that the electrode assembly was made airtight, thus preventing air leak into the discharge region. The x axis denotes the direction of the gas flow and the z axis denotes the direction normal to the electrode surface. The electrical characteristics of the discharge were studied by measuring the discharge voltage and the rf current as a function of time. The line-averaged spectral emission was monitored either by a photomultiplier (PM) tube or a CCD, fitted with collimators. In addition, the absolute concentration of ozone was measured by UV absorption of a Hg 253.6 nm line emission from a mercury lamp, assuming a cross section of $1.1 \times 10^{17} \, \mathrm{cm}^2$.[13]

Experimental measurements that characterize the APPJ discharge are shown in Figs. 1(b)–1(d). The measurements were taken for a pure helium discharge with an input power of 125 W and a gas flow rate of 50 slpm. Under these conditions, the temperature of the effluent gas was 70 °C at 0.5 cm past the end of the electrode. In Fig. 1(b) the intensity of
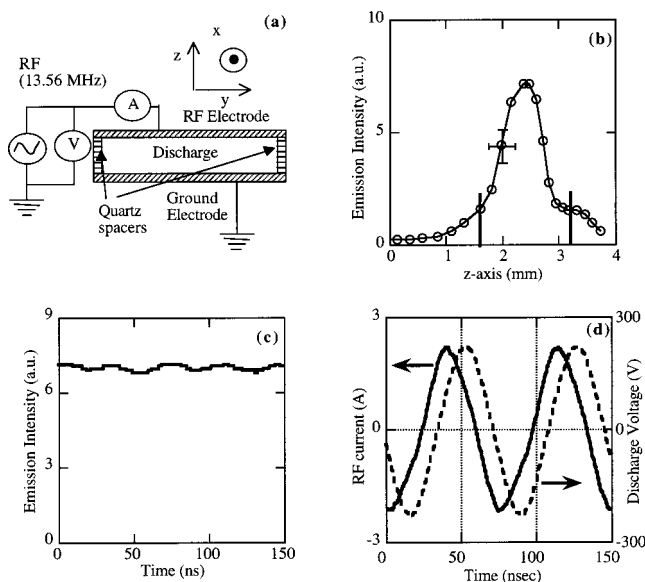
[a] Electronic mail: jypark@lanl.gov

FIG. 1. A schematic of experimental system and results. (a) Schematic of experimental system; (b) intensity of He I 706.5 nm emission (a.u.) as a function of position in *z* direction. The solid lines indicate the electrode locations. The observed emission signal outside of the electrodes is due to the stray light; (c) the intensity of He I 706.5 nm emission as a function of time; (d) waveforms of the rf current (solid) and the discharge voltage (dashed). Data are taken for helium discharge with an input power of 125 W, gap spacing of 0.16 cm, electrode dimension of 10 cm×10 cm, and gas flow rate of 50 slpm.
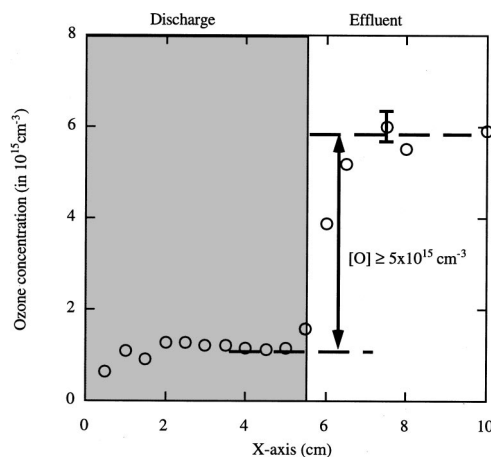

FIG. 2. Ozone concentration of the APPJ discharge and the estimate of the oxygen atom concentration. Input parameters are gas mixture of 99% helium and 1% oxygen at a flow rate of 50 slpm, input power of 200 W, gap spacing of 0.16 cm, electrode dimension of 5.5 cm×10 cm.

the He I 706.5 nm emission is shown as a function of position in the *z* direction, showing a volumetric discharge between the electrodes. In addition, the emission intensity of the same He I line is nearly constant in the *x* direction within the electrode length, while there is virtually no emission outside the discharge region due to very rapid electron cooling. Figure 1(c) shows the intensity of the He I 706.5 nm emission measured by a PM tube from the midsection of the discharge as a function of time. The rise time of the PM tube was 2.3 ns and the RC time of the amplifying circuit was 12 ns, while the radiative lifetime of the He I 706.5 nm emission is 56 ns. Thus, the nearly constant emission intensity indicates that the discharge is homogeneous in time, as the discharge parameters do not change appreciably during a rf cycle. In Fig. 1(d), the electrical property of the discharge is shown as a function of time. The rms amplitude of the discharge voltage is 156 V and the rf current is 1.6 A. The two waveforms are smooth, consistent with the temporally uniform emission from the discharge. In addition, the nearly sinusoidal waveforms indicate a mostly linear response of the discharge, while the capacitive nature of the APPJ discharge is clearly demonstrated by the current waveform leading the voltage waveform.

Practical usage of the APPJ discharge in materials applications depends critically on the production of the chemically active species. Figure 2 shows the absolute concentrations of ozone produced inside and outside the APPJ discharge. The measurements were obtained in the APPJ discharge using 1% oxygen in helium (input power of 200 W and gas flow of 50 slpm). For this measurement, the electrode length was shortened to 5.5 cm, followed by a collimated region (4.5 cm long) to maintain the uniform gas flow. In the discharge, ozone is produced by the reaction between

an oxygen atom and an oxygen molecule and destroyed mostly by the electron impact dissociation. Outside the discharge region, however, the electron impact dissociation becomes insignificant as the electrons lose their energy very quickly and recombine with ions. Consequently, the ozone concentration rapidly increases outside the discharge region as shown in Fig. 2. By comparing the ozone concentration in and outside the discharge region, the lower bound of atomic oxygen concentration in the discharge was found to be 5×10^{15} cm^{-3} since the formation of ozone requires oxygen atoms. This result shows that the APPJ produces a large concentration of oxygen atoms which has important value in many materials applications. Furthermore, the relative ratio of [O] and [O$_3$] in the APPJ source shows that the gas-phase chemistry in the APPJ discharge is much different from other atmospheric pressure plasma sources, e.g., the corona and dielectric barrier discharges, and is better suited for materials processing.[4,5]

To elucidate the underlying physics of the APPJ, a physical model was developed for a helium discharge. The model employs 1D two-moment fluid equations coupled with the Maxwell's equation and is based on the closure provided by the ''local field approximation.'' [14] The local field approximation assumes that the electron distribution function will be in equilibrium with the field both locally in time and space. The use of the local field approximation can be justified by the frequent collisions between charged particles and neutrals at atmospheric pressure. Fluid models based on the local field approximation have been employed in studies of high pressure plasma discharges, such as ac plasma display panel cells and dielectric barrier discharges, as well as low pressure rf glow discharges.[15–17]

Figure 3 shows a model result for a rf current density of 0.016 A (rms) cm^{-2} which corresponds to an input power density of 6.3 W cm^{-3}. The voltage waveform, shown in Fig. 3(a) is smooth and nearly sinusoidal, indicating a mostly linear response. The amplitude of the voltage waveform is 390 V and the phase difference is 77° with the current waveform preceding the voltage waveform. Temporal variation of the electron and ion density, in Fig. 3(b) shows that the electrons follow the instantaneous electric fields, while the ion
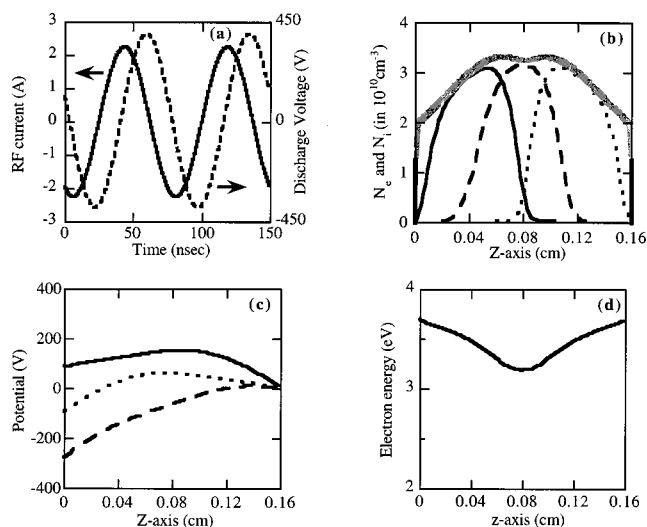
FIG. 3. Model results from a discharge with a rf current density of 0.016 A(rms) cm^{-2}. The input parameters are the secondary electron emission coefficient of 0.3 and gas temperature of 100 °C at 600 Torr (the atmospheric pressure in Los Alamos). (a) Waveforms of the rf current (solid) and the discharge voltage (dashed); (b) temporal variation of electron and ion density. From left to right, the electron density at $t = 0$ in solid line, at $t = 12$ ns in dashed line, and at $t = 38$ ns in fine dashed line. The ion densities at these various times are shown in thick gray lines; (c) temporal variation of electrostatic potential (the same line designation in electron density); (d) time averaged electron characteristic energy.

with the inefficient energy transfer between electrons and neutrals. Conversely, in the atmospheric pressure arc discharge, the high electron density, $10^{14} - 10^{16}$ cm^{-3}, heats the gas to a much higher temperature, typically above 3000 °C. In addition, the characteristic electron energy from the model also shows that the APPJ is well suited for producing a large concentration of atomic oxygen and maintaining a low ozone concentration in the discharge.

In summary, the APPJ discharge is fundamentally different from other atmospheric pressure plasma sources and can offer critical advantages for materials applications. The APPJ discharge is volumetric and homogeneous, and produces a large quantity of oxygen atoms at a gas temperature below 300 °C. A theoretical model confirms the existence of a stable discharge region and provides estimated electron densities of $0.2 - 2 \times 10^{11}$ cm^{-3} and characteristic electron energies of 2–4 eV. These plasma parameters indicate the unique advantage of the APPJ for producing a large quantity of chemically active species while maintaining a nonthermal discharge.

motion is governed mostly by the time-averaged electric fields. Also, the formation of a sheath, characterized by a depletion of electrons, and its motion is clearly shown in Fig. 3(b). The oscillating quasi-steady state solution is consistent with the APPJ discharge and demonstrates the existence of a stable and volumetric discharge at atmospheric pressure. In Fig. 3(c) the electrostatic potential variation shows that the transition between the sheath and the bulk region is smooth without a definitive boundary. This smooth transition is due to very frequent collisions between the charged particles and neutrals at atmospheric pressure.[18] When averaged over a rf cycle, the characteristic energy of the electrons is 3–4 eV in the discharge, as shown in Fig. 3(d). According to the model, the electron density increases from 0.2 to 2×10^{11} cm^{-3} for input power densities of 3–30 W cm^{-3} with little change in the characteristic electron energy. This moderate electron density explains the low gas temperature of the APPJ along

[1] D. M. Manos and D. L. Flamm, *Plasma Etching: An Introduction* (Academic, New York, 1989).
[2] V. N. Kolesnikov, Tr. Fiz. Inst. Akad. Nauk SSSR **30**, 66 (1964).
[3] Y. P. Raizer, *Gas Discharge Physics* (Springer, Berlin, 1991).
[4] R. S. Sigmond, *Electrical Breakdown of Gases*, edited by J. M. Meek and J. D. Craggs (Wiley, Chichester, 1978).
[5] B. Eliasson and U. Kogelschatz, IEEE Trans. Plasma Sci. **19**, 1063 (1991).
[6] H. Koinuma, H. Ohkubo, T. Hashimoto, K. Inomata, T. Shiraishi, A. Miyanaga, and S. Hayashi, Appl. Phys. Lett. **60**, 816 (1992).
[7] J. R. Roth, *Industrial Plasma Engineering: Vol. I, Principles* (Institute of Physics, Bristol, 1995), pp. 453–461.
[8] A. Schütze, J. Y. Jeong, S. E. Babayan, J. Park, G. S. Selwyn, and R. F. Hicks, IEEE Trans. Plasma Sci. **26**, 1685 (1998).
[9] J. Y. Jeong, S. E. Babayan, V. J. Tu, J. Park, R. F. Hicks, and G. S. Selwyn, Plasma Sources Sci. Technol. **7**, 282 (1998).
[10] S. E. Babayan, J. Y. Jeong, V. J. Tu, J. Park, G. S. Selwyn, and R. F. Hicks, Plasma Sources Sci. Technol. **7**, 286 (1998).
[11] J. Y. Jeong, S. E. Babayan, A. Schütze, V. J. Tu, J. Park, I. Henins, G. S. Selwyn, and R. F. Hicks (unpublished).
[12] H. W. Herrmann, I. Henins, J. Park, and G. S. Selwyn, J. Vac. Sci. Technol. A **17**, 2581 (1999).
[13] E. C. Y. Inn and Y. Tanaka, J. Opt. Soc. Am. **43**, 870 (1953).
[14] J. Park, D. Shim, C. S. Chang, and G. S. Selwyn (unpublished).
[15] J. Meunier, Ph. Belenguer, and J. P. Boeuf, J. Appl. Phys. **78**, 731 (1995).
[16] F. Massines, A. Rabehi, P. Decomps, R. B. Gadri, P. Segur, and C. Mayoux, J. Appl. Phys. **83**, 2950 (1997).
[17] J. P. Boeuf, Phys. Rev. E **36**, 2782 (1987).
[18] K. U. Riemann, Phys. Plasmas **4**, 4158 (1997).